Congress on Numerical Methods in Engineering 2011
Coimbra, 14 to 17 June, 2011

NUMERICAL AND EXPERIMENTAL REAL SCALE MODELLING OF AERODYNAMIC COEFFICIENTS FOR AN HIGH-PERFORMANCE VEHICLE

José C. Páscoa[1]*, Nelson M. Mendes[1], Francisco P. Brójo[2], Fernando C. Santos[1], Paulo O. Fael[1]

1: Electromechanical Eng. Department
2: Aerospace Sciences Department

Universidade da Beira Interior, Faculdade de Engenharia

Calçada Fonte do Lameiro, 6200-001, Covilhã, Portugal

e-mail: {pascoa,brojo, bigares, pfael}@ubi.pt; nelsonmendes07@gmail.com

Keywords: numerical modelling, experimental modelling, vehicle aerodynamics

Abstract. *Numerical modelling of high-performance road vehicles, in low-Re number conditions, undergoes a lack of accuracy usually associated to the use of RANS turbulence closures in these flow regimes. The usual assumption of developing experimental testing in reduced scale models hinders design targets, in view of the limitations associated to viscous scale effects. Herein we present an on-road real scale experimental testing, and the corresponding numerical modelling of the real geometry, for the UBI Eco-marathon vehicle. Aerodynamic coefficients are sought experimentally by towing the vehicle, while rolling resistance is obtained by shielding the vehicle to eliminate aerodynamic effects. An initial calibration of the numerical code is carried out using the Ahmed body test case as a benchmark. A detailed analysis of mesh influence on numerical accuracy is accomplished. By using this knowledge base, a numerical computation is performed for the high-performance vehicle. The computed flowfield results, obtained for the UBI Eco-marathon vehicle, provide valuable indications on how to improve the aerodynamic behaviour. These conclusions are now being incorporated in the new version of the vehicle.*

1. INTRODUCTION

Traditionally, studies on ground vehicle aerodynamics where mostly performed using experimental techniques and also, lately, by means of Computational Fluid Dynamics (CFD). Both approaches present difficulties in achieving a real scale modelling of vehicle aerodynamics in the road conditions [1,2]. However, the precise modelling of the different resistance coefficients for a vehicle operating on real road conditions is of paramount importance. Among these coefficients we consider, mainly, aerodynamic and rolling resistance, with other minor variables, such as transmission and suspension losses, still existing. Their importance connects to the need to evaluate realistically the vehicle performance. Among the on-road experimental techniques used to determine resistance coefficients the most common is the coast-down method, which is usually hindered by non-constant test conditions being either due to cross-wind or to road lane non-uniformity. The use of wind-tunnels for experimental testing introduces blockage effects and difficulties in achieving Reynolds number similarity, along side with the problem associated to the accurate modelling of tyre-road interaction [3]. Alternatively, a computational approach based on CFD as seen remarkable progress. Nevertheless, it's usefulness to model real geometries of ground vehicles has been difficult to demonstrate, in part due to numerical turbulence model weaknesses and also due to the complexity of the vehicle's geometry involved. The increasing availability of computer power, and the improvement in numerical models, made it possible to trust on CFD to model the flow in complete real scale ground vehicle geometries.

Initially, in order to circumvent all the problems associated to a realistic modelling of road vehicles, the use of simplified experimental and numerical models was the adequate approach [4,5,6]. This allowed an increase on the performance of these vehicles over time. Even if not giving an absolute and totally accurate value for the aerodynamic coefficients, the use of wind tunnel data and RANS on simplified geometries conducted the designers in the right track to improve the vehicle’s performance, either it be for dynamic stability or for achieving a reduction in fuel consumption. A similar approach was also applied to study vehicle air intakes, in order to improve cooling performance, with remarkable results.

Although useful to get an insight into the adequate design trend, for performance improvement, the use of CFD for ground vehicle aerodynamic studies resulted in discrepancies between the numerical values obtained by diverse authors, for the same geometry, with the same situation occurring with experimental results. This is true even for very simple model geometries, such as the Ahmed body [7,8]. The issues impacting the usefulness of CFD predictions are the meshing strategy, turbulence modelling and realistic turnaround time. As most of drag losses occur in a detached wake behind the vehicle then a refined turbulence modelling must be considered in that region. Actually, the capability to accurately predict the wake became a selective criterion to consider the accuracy of turbulence modelling. This is one of the reasons why we have introduced the Ahmed body initially, before the Shell Eco-marathon real vehicle.

As already stated we rely on the solution of the Reynolds-Averaged Navier-Stokes equations in conjunction with turbulence models. More recently there have been efforts to

apply Large Eddy Simulation to generic car bodies, these have been fraught with difficulties that arose from the extremely high computational resources required at the high Reynolds numbers involved [7]. These problems are associated with the highly constraining grid requirements, especially in the near wall region. More realistic for every day design efforts is the alternative of applying unsteady RANS, because of their certain impact on the dynamics of the large-scale energetic fluid motion in massive separation, with this reasoning being related to the presence of a strong flow instability in the form of a periodic shedding. Such vortex shedding can appear in the wake of bluff bodies, but the main separation process from the streamlined main flowfield, such as in the slanted rear window of an Ahmed body, is not necessarily due to this vortex shedding [9,10]. This introduced the question; What can be achieved in the computation of separated ground-vehicle flows by the use of advanced turbulence closures, within a steady state framework, as compared to on-road aerodynamic vehicle tests. The answer to this question is the main subject of the present work.

2. NUMERICAL MODEL

The numerical computations were performed through the Ansys Fluent commercial code, we solve the Reynolds-Averaged Naviers-Stokes equations for steady-state, including an adequate turbulence model.

Several turbulence closures were considered, such as k-ε RNG, Spalart-Allmaras and k-ω SST. Previous studies concluded that k-ε RNG is superior to the standard k-ε model in what refers to the prediction of drag coefficient and pressure distribution, with the k-ω SST presenting the best accuracy [7]. We have used an unstructured mesh, with the grid not being aligned with the flow, therefore a second-order spatial discretization is of paramount importance. Usually, and in order to ensure a faster convergence, the test-cases were converged with first-order discretization before switching to second-order. The near wall grid count was constructed in order to use a wall-function approach, even if we are using a low-Re turbulence closure. The imposed boundary conditions for all numerical results presented in this work are: a) a uniform velocity inlet with a 0.25% turbulence intensity and a turbulent length scale of 1% of vehicle height; b) an outlet flow boundary condition; c) a constant far-field velocity imposed in the lateral and top evolving boundaries; d) a no-slip solid wall boundary condition in the vehicle body and ground; e) a rotating wall boundary condition in the vehicle tyres.

3. COMPARISON BETWEEN NUMERICAL AND EXPERIMENTAL RESULTS

The numerical computations started by analysing the flow in the Ahmed body test case, see Fig. 1. This case was chosen in order to get acquainted with the numerical difficulties associated to the modelling of ground vehicle aerodynamics. By using a test case that has been studied by several authors, both experimentally and numerically, we can ensure the comparison between our numerical results and those of others, thus ensuring a knowledge-base to overcome the difficulties associated to the realistic modelling of the eco-marathon vehicle. Both geometries are enclosed inside a virtual wind-tunnel box whose entrance boundary is at a distance of 5 times the vehicle length. Being the other box-boundaries at 5

times the vehicle size in vertical and lateral directions. We have also obtained results with 10 times longer distances, but the drag coefficient values did not altered significantly. We thus present in the present work the reduced boundary results, in a following work we intent to present a more detailed analysis on the boundary distance effect onto the computed drag coefficient.

3.1 Numerical results for the Ahmed body

The Ahmed body was tested with diverse mesh densities and various block topologies. Two meshes, one with 487 323 nodes and another with 1 185 028 nodes in a single block, also two more with 261 487 nodes and 1 256 563 nodes comprising two blocks each, and finally two additional meshes having 150 956 nodes and 802 413 nodes in a three block distributed topology. The diverse meshes where tested for two main parameters, being it the cell skewness and the y^+ in the near wall region. The bad skewness values occurred mainly in the under body, in the supporting stilts of the Ahmed body. Regarding the y^+, its normalized values must be comprised between 30 and 300, this resulted difficult to achieve in the back side of the body, see Fig. 2-a).

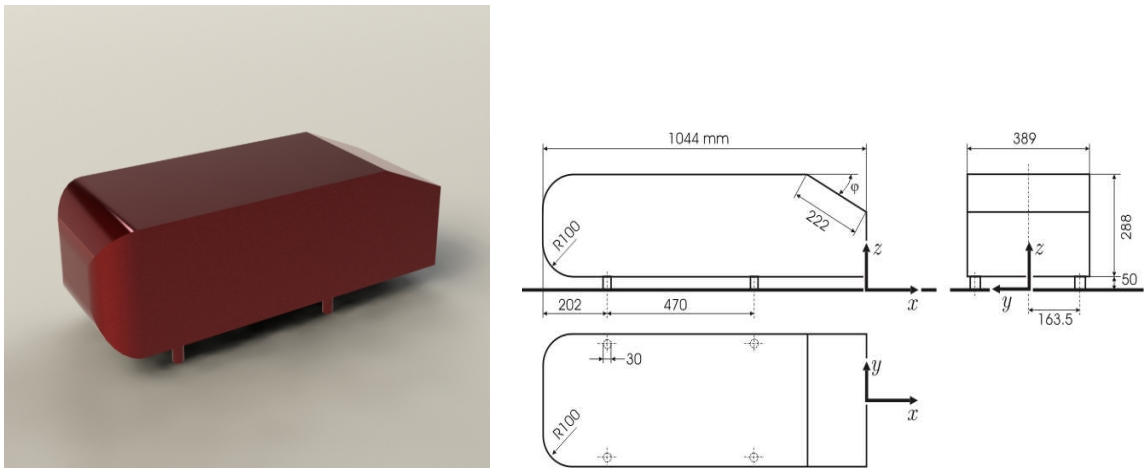

Figure 1: Layout of Ahmed body, from Solidworks, and geometric dimensions used to define the test-case; all dimensions are in [mm]. Flow direction is from left to right [4].

The analysis of the behaviour of the flow on the Ahmed body can be done by looking at integral quantities such as lift and drag, or alternatively by looking into the detailed flow pattern. The initial analysis of the results was done by comparing the drag coefficient from our numerical computations with the open literature. We have obtained a Cd=0.30633 from our numerical computations, and this compares well with a Cd=0.2948 described in [4], see Table 1. It is not uncommon to find slightly different values in the literature. The origin of the scatter in experimental results comes from the various experimental testing conditions; these being diverse wind tunnel turbulence intensities or blockage effects. We can also notice that for the Cd=0.30633=0.2546 (pressure drag) + 0.0517 (viscous drag).

	Cd		
	V= 30 m/s	V= 40 m/s	V=60 m/s
1 185 028 nodes (1B)	0.30633	0.30401	
150 956 nodes (3B)	0.31103	0.30825	
Experiment [4]			0.2948

Table . Results obtained for drag coefficient and comparison to experimental value.

As previously stated, the drag coefficient is strongly dependant upon the flowfield on the rear slanted window. According to [10], the flow in this back area of the body is characterized by two main components. First, the occurrence of two large vortices that develop in the main flow direction being originated at the two top rear lateral corners, in the roof junction between the lateral walls and the slanted window. A second component that is related to a boundary layer separation, immediately followed by reattachment, that can take place in the slanted window. This later forms a kind of separation bubble, the occurrence of this flow feature is strongly dependant upon the slant angle, in our case the turbulent mixing rate in the body roof boundary layer is enough to almost prevent separation in the roof top edge, at the slat beginning, by resisting the adverse pressure gradient. We can see that we didn't capture any separation bubble in the slanted surface, but only a massive separation in the back body face, see Fig 2-b). According to [6], and for a slanted angle of 25º, there is no laminar separation bubble in the slanted surface, thus agreeing with our results.

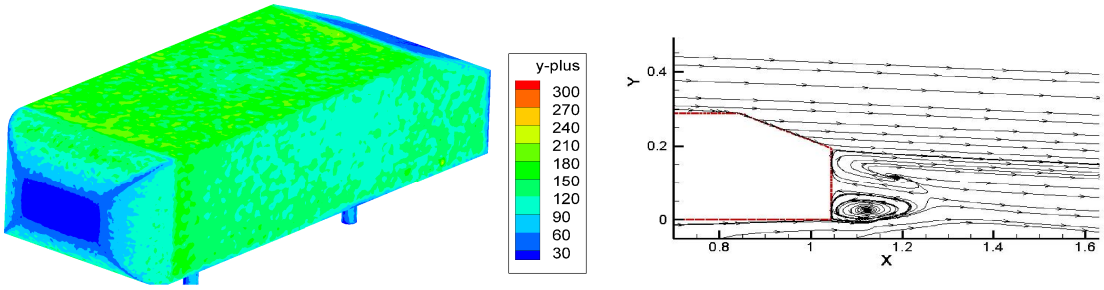

a) b)

Figure 2: Results from the numerical simulations at V=30 m/s (Re=2x10^6) with a turbulence intensity 0.25%xV and Le= 1% of vehicle height. a) distribution of y^+ on the body solid surface. b) Stream-traces in the body's center-plane. These compare qualitatively well, there is no separation bubble, with the results presented in [6] for the same slanted angle of 25º.

A more detailed analysis can be made when comparing the numerical and experimental results for the pressure coefficient obtained by pressure tappings, see Fig. 3. This analysis is more difficult because we are in the near lateral edge. The direct comparison implies that the numerical results can capture adequately the strong vortex structure in that region. Also, the pressure tappings are constructed in order to obtain the mean pressure, thus

smoothing any unsteadiness from the experimental results. Further, the experimental results are only available for a corner of the slanted surface. We have compared in Fig. 3-a) the results of the pressure coefficient isolines, and these present some discrepancies. Albeit this, the major features are present in the numerical computations. A more detailed comparison was indeed attempted, in this case by looking at the pressure coefficient distribution on a slice of the slanted surface. This slice, in Fig. 3-b), is taken at 0.005 m from the lateral edge. We can see that the pressure peak obtained from the experiments is not in phase with the pressure peak obtained from the numerical computations. However, the pressure distribution agrees quite well in the remaining part of the slant surface.

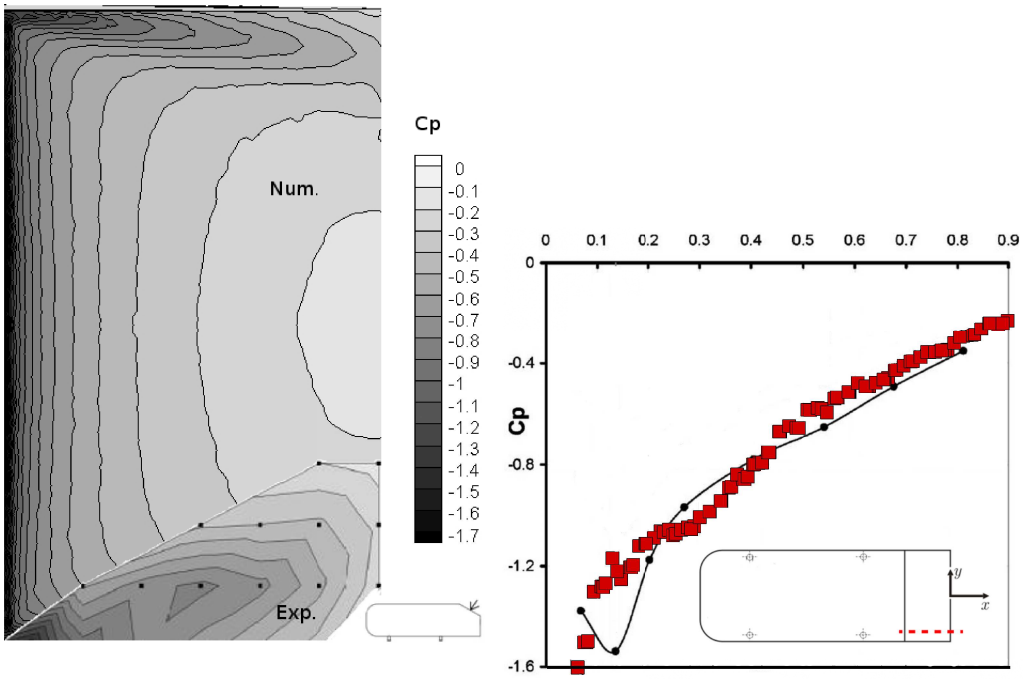

a) b)

Figure 3: Results from the numerical simulations at V=30 m/s (Re=2x10^6) with a turbulence intensity 0.25%xV and Le= 1% of vehicle height. a) Isolines of pressure coefficient obtained in the numerical and experimental computations, the experimental result is only presented for a corner of the slant face. b) Comparison between the experimental (circle) and numerical (square) pressure coefficient values. The experimental results where obtained on the dashed line that is parallel to the edge between the rear slant face and the rear side, located 0.005 m from the lateral edge [10].

The analysis of the flow on the Ahmed body allowed us to take into consideration the limitations in accuracy of the numerical model. Being these related to geometry discretization difficulties or associated to the deficiencies on the turbulence model assumptions. The classical comparison between experiments in wind tunnel and numerical computations is further complicated when we adress the on-road vehicle conditions. In the following section we will provide a comparison between the on-road and numerical computations for the Shell Eco-marathon vehicle.

3.2 Experimental and numerical results for the Eco-marathon vehicle

The results obtained for the Ahmed body are readily compared to diverse results presented in the literature, both experimental and numerical. However, for the eco-marathon vehicle we need to perform our own set of experiments. The vehicle was completely designed, and built, at University of Beira Interior. Albeit the main purpose of the Shell Eco-marathon contest is the reduced fuel consumption of the vehicle, the considered vehicle was mainly designed to compete in the aesthetically design competition. This resulted in a less performing vehicle due to the increased weight given to aesthetic options, producing a vehicle that can be used as a good test case for aerodynamic performance improvements. The use of coast-down methods is not adequate to determine the drag coefficient at these low Re conditions, in particular because it only gives a mean value for the drag coefficient. We must recall that numerical results are obtained for a single velocity, so we need to compare the drag coefficient at exactly that velocity. In order to being able to compute a velocity dependent drag coefficient a different technique was implemented [3]. We have conducted a constant velocity test by towing the test vehicle with a shield, to remove aerodynamic component drag, see Fig 4. In the following tests we towed the vehicle unshielded in order to obtain the total drag, with the aerodynamic component being readily obtained by subtracting the rolling resistance obtained in the former shielded tests.

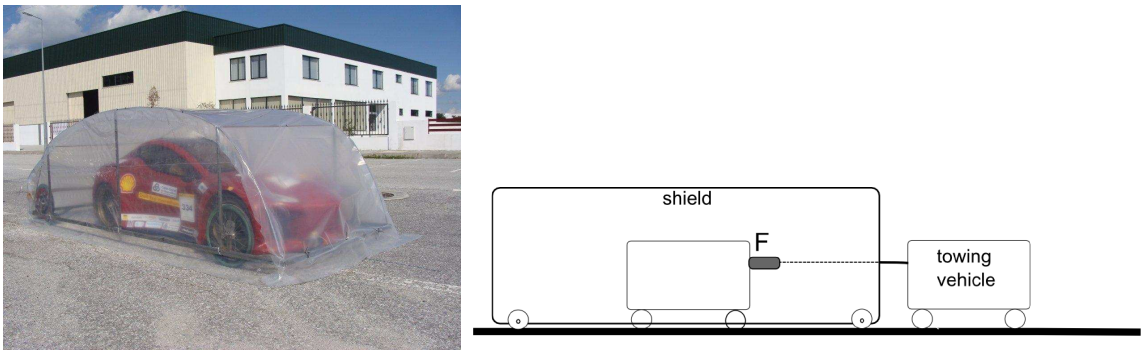

Figure 4: Experimental on-road constant velocity test. Initially the vehicle is shielded in order to determine the rolling resistance component. The total resistance is obtained in subsequent tests using a towing vehicle at a distance 10 times the test vehicle length, to reduce towing vehicle interference.

The Eco-marathon vehicle requires a very detailed geometric model, 400 000 nodes. In order to accomplish this, particularly in the tyre and under body region a very fine surface mesh was introduced. In the numerical computation we have implemented a relative velocity boundary condition for the rotating tyres. This condition introduces the tyre spinning with an angular velocity centred at the wheels axis. The results obtained from the experiments are Cd=0.43 and from the numerical computations are Cd=0.4662=0.4353 (pressure drag) +0.0309 (viscous drag). Discrepancies are due to experimental errors and to numerical inaccuracies, see Fig. 5. Major sources of experimental error are due to difficulties associated to maintain a constant velocity during the on-road testing.

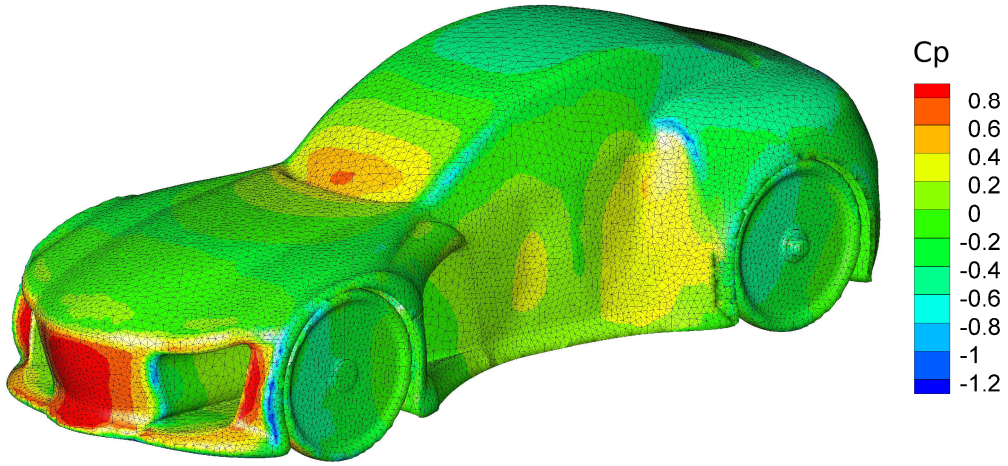

a)

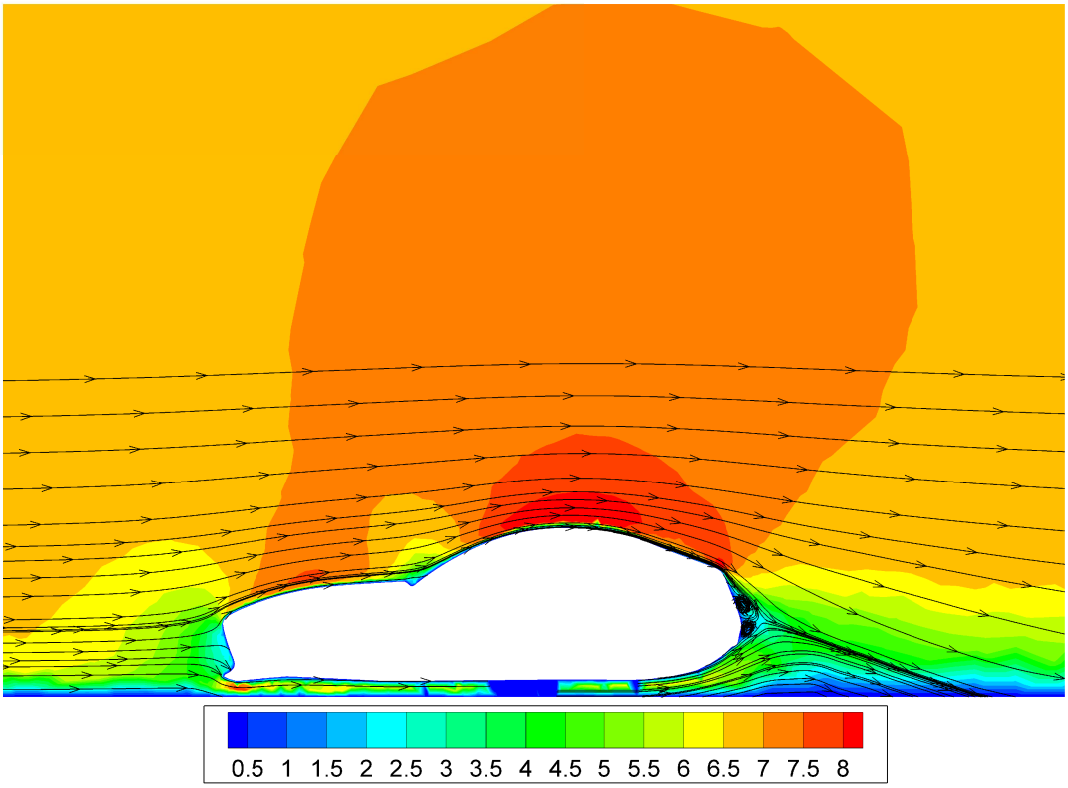

b)

Figure 5: Numerical results for the Shell Ecomarathon vehicle. a) Pressure coefficient and b) streamlines and mean velocity (m/s) at a mid-section of the vehicle.

Numerical inaccuracy is mostly related to a precise geometric detail modelling and to the lack of accuracy of k-ω SST turbulence model in these low-Re conditions, in particular due to boundary layer transition modelling.

By looking at Fig. 5-a) we can visualize the vehicle's surface areas with significant values of stagnation pressure. These areas are visible in the vehicle front face and also in the lateral surfaces just behind the doors. Further, the vehicle includes two tunnels in the lateral zones near the front wheels. These two tunnels are the source of additional viscous and mixing losses. We also present a mid-section plane of the vehicle, in Fig. 5-b). We can see that the upper surface of the vehicle is quite streamlined. The trailing edge vortex shedding has been reducing by a careful design, by UBI team, of the rear portion of the under-surface of the vehicle.

4. CONCLUSIONS

The comparison between wind tunnel experimental results and numerical computations is quite routinely presented in the literature for ground vehicle aerodynamics. The results are usually very precise when we compare integral quantities, such as drag coefficient. This same conclusion can be drawn from the results we have obtained for the Ahmed body. However, a reduced accuracy is achieved when we compare local pressure or velocity distributions. Albeit this, it is very difficult to achieve a realistic modelling of road vehicles in wind tunnel.

To be able to compare the numerical results for the Shell Ecomarathon vehicle with experiments we have performed on-road measurements. These experiments are very prone to repeatability errors and have been performed with great care. We concluded that the numerical and experimental results compare with lower accuracy than the ones obtained for the Ahmed body. Albeit this, the investigation carried out in the present work is very useful to understand the aerodynamic loss generation mechanism in the Eco-marathon vehicle. Both, the numerical, and experimental, values obtained for the drag coefficient are much higher that the values expected for this kind of vehicles. The reason being, mainly, because the presented vehicle was designed to compete in the aesthetic category, with no strong concern for aerodynamic performance. Incidentally, this resulted in an excellent test case to perform research on aerodynamic flow optimization.

ACKNOWLEDGEMENTS

The authors would like to thank the support from CAST-Centre for Aerospace Sciences and Technology, FCT Research Unit No. 152, from University of Beira Interior.

REFERENCES

[1] M. E. Biancolini, F. Renzi,G. Manieri and M. Urbinati, *Evaluation of aerodynamic drag of go kart by means of coast down test and CFD analysis,* Associazione Italiana per l'Analisi delle Sollecitazioni (AIAS), *XXXVI Convegno Nazionale*, Napoli (2007), pp. 1-13.

[2] G. Le Good, J. Howell, M. Passmore and A. Cogotti, *A comparison of on-road*

aerodynamic drag measurements with wind tunnel data from Pininfarina and MIRA, Society of Automotive Engineers, Developments in Vehicle Aerodynamics 1998 (SP-1318), SAE paper 980394, pp. 1-9.

[3] J. Chua, F. Fuss and A. Subic, "Rolling friction of a rugby wheelchair", *Procedia Engineering* Vol. **2**, pp. 3071-3076, (2010).

[4] S. R. Ahmed, G. Ramm and G. Faltin, *Some salient features of the time-averaged ground vehicle wake*, Society of Automotive Engineers (1984), SAE paper 840300.

[5] G.. Le Good and K. Garry, *On the use of reference models in automotive aerodynamics*. Society of Automotive Engineers, Vehicle Aerodynamics 2004 (SP-1874), *SAE paper 2004-01-1308,* pp. 1-25.

[6] H. Lienhart and S. Becker, *Flow and turbulence structure in the wake of a simplified car model, Society of Automotive Engineers (2003), SAE paper 2003-01-0656.*

[7] T. Nakashima, M. Tsubokura, T. Nouzawa, T. Nakamura, H. Zhang and N. Oshima, *Large-Eddy simulation of unsteady vehicle aerodynamics and flow structures*. BBAA VI International Colloquium on: *Bluff Bodies Aerodynamics & Applications*, Milano, Italy (2008), pp. 1-14.

[8] H. Choi, W.-P. Jeon and J. Kim, "Control of Flow Over a Bluff Body", *Annual Review of Fluid Mechanics* Vol. **40**, pp. 113-139, (2008).

[9] C.-H. Bruneau, E. Creusé, D. Depeyras, P. Gilliéron and I. Mortazavi, "Coupling active and passive techniques to control the flow past the square back Ahmed body", *Computers & Fluids* Vol. **39**(10), pp. 1875-1892, (2010).

[10] P. Gillieron, A. Leroy, S. Aubrun and P. Audier, "Influence of the Slant Angle of 3D Bluff Bodies on Longitudinal Vortex Formation", *Journal of Fluids Engineering* Vol. **132**, pp. 051104-1-051104-9, (2010).